Chaos, Solitons and Fractals 78 (2015) 194–204

Contents lists available at ScienceDirect

Chaos, Solitons and Fractals

Nonlinear Science, and Nonequilibrium and Complex Phenomena

journal homepage: www.elsevier.com/locate/chaos

Effect of magnetic field on the radial pulsations of a gas bubble in a non-Newtonian fluid

S. Behnia [a,*], F. Mobadersani [b], M. Yahyavi [c], A. Rezavand [d], N. Hoesinpour [b], A. Ezzat [e]

[a] Department of Physics, Urmia University of Technology, Urmia, Iran
[b] Department of Mechanical Engineering, Urmia University, Urmia, Iran
[c] Department of Physics, Bilkent University, Ankara 06800, Turkey
[d] Department of Mechanical Engineering, Iran University of Science and Technology, Tehran, Iran
[e] School of Computer Engineering, Nanyang Technological University, Singapore

ARTICLE INFO

Article history:
Received 27 October 2014
Accepted 28 July 2015
Available online 1 September 2015

Keywords:
Bubble dynamics
Nonlinear acoustics
Viscoelastic
Bifurcation diagrams
Lyapunov spectrum

ABSTRACT

Dynamics of acoustically driven bubbles' radial oscillations in viscoelastic fluids are known as complex and uncontrollable phenomenon indicative of highly active nonlinear as well as chaotic behavior. In the present paper, the effect of magnetic fields on the non-linear behavior of bubble growth under the excitation of an acoustic pressure pulse in non-Newtonian fluid domain has been investigated. The constitutive equation [Upper-Convective Maxwell (UCM)] was used for modeling the rheological behaviors of the fluid. Due to the importance of the bubble in the medical applications such as drug, protein or gene delivery, blood is assumed to be the reference fluid. It was found that the magnetic field parameter (B) can be used for controlling the nonlinear radial oscillations of a spherical, acoustically forced gas bubble in nonlinear viscoelastic media. The relevance and importance of this control method to biomedical ultrasound applications were highlighted. We have studied the dynamic behavior of the radial response of the bubble before and after applying the magnetic field using Lyapunov exponent spectra, bifurcation diagrams and time series. A period-doubling bifurcation structure was predicted to occur for certain values of the parameters effects. Results indicated its strong impact on reducing the chaotic radial oscillations to regular ones.

1. Introduction

The dynamics of bubble formation and collapse have been studied using a number of publications, including the studies of radial oscillating bubbles by Rayleigh [1], Plesset [2,3], Crum et al. [4], Flynn [5], Lauterborn [6], Plesset et al. [7], Prosperetti [8–10] and so on. Therefore, it is important to develop a technique in order to study the bubble radial stability in distinctive situations. In view of the escalating use of the bubbles in new applications, particularly medical and industrial, the number of studies on the growth and collapse of the bubbles in different structures and environments has increased [11]. In more important medical applications, bubbles are used for the delivery of drugs [12–14], cancer treatment [15–17], and the barrier opening of clogged veins and arteries [18,19]. In all cases, bubbles should move and grow in the blood stream and collapse in the intended location. So it is important to take the bubbles radius motion stable and not permit to collapse until the required region. The research conducted on blood indicates that approximation blood rheology by non-Newtonian models, correlates well with the experimental results [20,21].

Therefore, the study of bubble growth and its stability in non-Newtonian fluid will be of the most important concern [22]. The chaotic behavior of bubbles moving in a

* Corresponding author. Tel.: +98-9141468515.
E-mail address: s.behnia@sci.uut.ac.ir, behniasohra4@gmail.com (S. Behnia).

http://dx.doi.org/10.1016/j.chaos.2015.07.029
0960-0779/

non-Newtonian fluid has been investigated experimentally by Jiang et al. [23]. In addition to experimental studies [24–27], there have also been many theoretical investigations on bubble growth [28–32]. In the article presented by Wang et al. [33], the nonlinear vibration of a protein bubble submerged in bingham liquid has been mathematically modeled, and the bubble's reaction to pressure pulses has been studied. By presenting an analytical model for bubble growth in linear viscoelastic fluids and solving it through the perturbation method, Allen et al. [34] showed that the increase in the Deborah number leads to an increase in bubble radial oscillation amplitude. Deborah number is a non-dimensional elastic parameter which is defined as the ratio of the relaxation time and characteristic timescale for the bubble radius oscillation [34]. In another article, Allen et al. [35] extended his analytical model to nonlinear, non-Newtonian fluid (UCM fluid) and used numerical methods to solve the integro-differential equations. They have also demonstrated the increase in bubble radial oscillation amplitude with the increase in the Deborah number. In the work of Jimenez-Fernandez [36], through the development of analytical relations for bubble growth in non-Newtonian fluid fields affected by the external pulses, the growth of bubbles under the influence of factors like pulse intensity, the Reynolds number and the amount of elasticity has been investigated. In this study, it has been emphasized that with the increase in the Deborah number, bubble growth will become chaotic, and the bubble will approach the state of collapse.

Furthermore, in different theoretical studies, the subject of bubble growth in non-Newtonian fluid showed that in cases where the Reynolds number is of the order 1, the growth and collapse of bubbles can be controlled via Newtonian viscosity. Lind and Phillips [37] have demonstrated the growth of bubbles in non-Newtonian fluids through different constitutive equations. According to their results, at large Deborah numbers, a bubble displays a completely elastic behavior, and its energy diagram indicates a rebound in bubble growth. Brujan et al. [38] used the perturbation method to study the growth of bubbles in non-Newtonian compressible fluids. They showed that at larger Reynolds numbers, sound emission plays the major role in the damping of bubble radial oscillations. Also because of the importance of bubble dynamics, several studies have been conducted on the subject of bubble stability. That is, when the bubble motion gets chaotic, its behavior becomes unpredictable and difficult to deal with [39,40]. In this case, the chaotic nature of the equation requires particular tools for resolution because of the inadequacy of the analytical and linear solutions. By using the primary theory of dynamic systems, Bloom [32] has presented the stable and unstable behaviors of bubbles in non-Newtonian fluids. Aliabadi et al. [41] examined the growth of bubbles in a non-Newtonian fluid field. They have demonstrated that the bubble radial oscillation amplitude decreases under the influence of a magnetic field. Building upon Bloom and Aliabadi's work, the enhanced understanding of the behavior of bubbles in non-Newtonian fluids as well as the ability to reduce the chaotic radial oscillations could be the first step in controlling the bubble dynamics.

The main argument of this study focuses on various aspects of the dynamics of bubbles in non-Newtonian fluids with the presence of magnetic fields. In addition, the effects of substantial parameters that influence the bubble dynamics are studied in a large domain using chaos theory and considering the measure of the non-Newtonian state of the fluid (Deborah number). Bifurcation and Lyapunov exponent diagrams [42–44] are presented for special cases to determine the chaotic regions. Comprehensive information is presented about extremely nonlinear pulsations of bubbles in non-Newtonian fluids at high amplitudes of acoustic pressure where deterministic chaos manifests itself in order to determine the stable and chaotic regions of the system, particularly for drug and gene delivery applications where the applied acoustic pressure is considerably greater than the pressure employed in the ultrasound imaging.

It has been shown that by imposing a radial magnetic field, the rate of growth and collapse of the bubbles dampens considerably. Increasing the magnitude of the magnetic field will cause an increase in the damping effect and, as a result, the growth and collapse of the bubbles can be controlled. The effects of magnetic fields, acoustic field properties and the Deborah number on stability of non-Newtonian fluids are discussed in the following sections.

2. Dynamics of spherical bubble in viscoelastic fluids

The governing equation of bubble growth in non-Newtonian fluid follows the general Rayleigh–Plesset (GRP) equation, and with regards to the viscoelastic effects of the fluid, the following integro-differential equation is obtained [35]:

$$R\ddot{R}+\frac{3}{2}\dot{R}^2=\frac{1}{\rho}\left[p_g-p_\infty-\frac{2\sigma}{R}+2\int_R^\infty\left(\frac{\tau_{rr}-\tau_{\theta\theta}}{r}\right)dr\right] \tag{1}$$

In the above equations, τ_{rr} and $\tau_{\theta\theta}$ are components of the shear stress tensor, which have a non-uniform field distribution because of the deformation that exists in the fluid field. Eq. (1) has been written for a bubble with radius R which is affected by a pressure field far away from the bubble, p_∞, in the form of $p_0+P_a\sin(\omega t)$, where p_0 is the ambient pressure. The pressure pulse enters the fluid field with angular frequency ω and pressure amplitude P_a. Also p_g and σ denote the uniform pressure inside the bubble and surface tension of the fluid, respectively. For simplicity, we assume that the internal gas follows a polytropic relationship with exponent k, and we have $p_g=p_{g_0}(\frac{R_0}{R})^{3k}$, where p_{g_0} and R_0 are the gas bubble pressure and the bubble radius at the initial equilibrium state respectively. By considering the UCM time derivative method [34,35], the radial and theta stress tensor terms will be obtained through the following simplified differential equations:

$$\begin{cases}\tau_{rr}+\lambda_1\left(\frac{\partial\tau_{rr}}{\partial t}+\frac{R^2\dot{R}}{r^2}\frac{\partial\tau_{rr}}{\partial r}+\frac{4R^2\dot{R}}{r^3}\tau_{rr}\right)=4\eta_0\frac{R^2\dot{R}}{r^3},\\ \tau_{\theta\theta}+\lambda_1\left(\frac{\partial\tau_{\theta\theta}}{\partial t}+\frac{R^2\dot{R}}{r^2}\frac{\partial\tau_{\theta\theta}}{\partial r}-\frac{2R^2\dot{R}}{r^3}\tau_{\theta\theta}\right)=-2\eta_0\frac{R^2\dot{R}}{r^3}.\end{cases} \tag{2}$$

where η_0 is the zero shear-rate viscosity, λ_1 is the relaxation time, and r is the distance of each element from the coordinate system's origin. By applying the perturbation method, Allen et al. [34,35] solved the above coupled equations and then, in 2001, they introduced the transformation $y=r^3-R^3(t)$ to immobilize the coordinate by using the Lagrangian

perspective where $y=0$ indicates the bubble boundary [35]. The upper limit of the integral in Eq. (1) should be selected in such a way that both terms of the shear stress tensor (radial and theta) become zero. Eq. (1) shows the growth of a bubble immersed in a non-Newtonian fluid, which oscillates at its dimensionless radius R under the influence of an external pressure pulse. Considering the magnetic field (B) in the calculations (See Appendix A), if the following definitions of the non-dimensional time, radius, radial spatial variable, stress and Reynolds number [35]

$$\bar{t}=\omega t;\quad \bar{R}=R/R_0;\quad \bar{r}=r/R_0;$$
$$\bar{\tau}=\tau\frac{R_0}{\eta_0}\sqrt{\rho/\rho_0};\quad Re=\frac{\rho\omega R_0^2}{\eta_0} \tag{3}$$

are used, the Rayleigh–Plesset Eq. (1) is written in non-dimensional form as

$$R\ddot{R}+\frac{3\dot{R}^2}{2}+\frac{\sigma B^2}{\rho}R\dot{R}=\frac{p_0}{\rho\omega^2R_0^2}\left[\left(1+\frac{2\sigma_s}{p_0R_0}\right)\left(\frac{1}{R}\right)^{3k}-\left(\frac{2\sigma_s}{p_0R_0}\right)\left(\frac{1}{R}\right)-(1+\alpha\sin(t))\right]+\frac{1}{Re}\frac{1}{\omega R_0}\sqrt{\frac{p_0}{\rho}}\times\int_r^{r_1}\left(\frac{\tau_{rr}-\tau_{\theta\theta}}{r}\right)dr \tag{4}$$

where α is the ratio of the acoustic forcing pressure amplitude to the ambient pressure, σ_s is the surface tension and σ is the liquid electrical conductivity. In dimensionless form, the stress tensor components Eq. (2) could be rewritten as

$$\begin{cases}\tau_{rr}+De\left(\frac{\partial\tau_{rr}}{\partial t}+\frac{R^2\dot{R}}{r^2}\frac{\partial\tau_{rr}}{\partial r}+\frac{4R^2\dot{R}}{r^3}\tau_{rr}\right)=4(\omega R_0\sqrt{\frac{\rho}{p_0}})\frac{R^2\dot{R}}{r^3},\\ \tau_{\theta\theta}+De\left(\frac{\partial\tau_{\theta\theta}}{\partial t}+\frac{R^2\dot{R}}{r^2}\frac{\partial\tau_{\theta\theta}}{\partial r}-\frac{2R^2\dot{R}}{r^3}\tau_{\theta\theta}\right)=-2\left(\omega R_0\sqrt{\frac{\rho}{p_0}}\right)\frac{R^2\dot{R}}{r^3}.\end{cases} \tag{5}$$

The Deborah number ($De=\lambda_1\omega$) is a dimensionless number which designates the time required for the fluid response divided by the flow pulse time, and in fact, it measures the non-Newtonian state of the fluid [35]. Since the constitutive equations used are based on the assumption that the fluid is incompressable, radiation damping is not considered (see Table 2 for parameter ranges).

3. Analysis tools

There are several mathematical tools available for quantifying bubble stability rang. The reasons for using maximum Lyapunov exponents and bifurcation structure in the absence of direct mathematical methods are:

- The maximum Lyapunov exponents, approximated computationally for a wide range of various values, clearly indicate the chaotic behavior of bubble dynamics.
- The computationally based bifurcation analysis illustrates that the bubble dynamics transit among different regions such as periodic, chaotic attractors and intermittent behavior.

3.1. Computation of Lyapunov exponents

The Lyapunov exponent is a quantitative measure of chaotic dynamics of a system by examining its very sensitive dependence on initial conditions. The Lyapunov exponents are defined as follows: consider two nearest neighboring points in phase space at time 0 and t, with distances of the points in the i-th direction $\|\delta x_i(0)\|$ and $\|\delta x_i(t)\|$, respectively. The Lyapunov exponent is then defined through the average growth rate λ_i of the initial distance,

$$\frac{\|\delta x_i(t)\|}{\|\delta x_i(0)\|}=2^{\lambda_i t}\quad (t\to\infty)$$
$$\text{or}\quad \lambda_i=\lim_{t\to\infty}\frac{1}{t}\log_2\frac{\|\delta x_i(t)\|}{\|\delta x_i(0)\|} \tag{6}$$

Using the estimation of local Jacobi matrices method, the Lyapunov exponent is calculated for a number of given control parameters. The value of each of the control parameters is then slightly increased, and the Lyapunov exponent is recalculated for each of them after the value increase. By doing this repeatedly, the Lyapunov exponent spectrum of the bubble dynamics system is plotted versus the control parameters. Recently, dynamic system theory has been applied in a comprehensive analysis of the nonlinear response of bubble [45,46].

3.2. Bifurcation diagrams

Period doubling, quasi-periodicity, and intermittency [47] are well known routes of transition from periodic to chaotic behaviors with their origins in local bifurcations. In this paper, the dynamic behavior of the bubble radial oscillations is studied by plotting the bifurcation diagrams of the normalized radius of the bubble after altering each of the different control parameters. The analysis of the bifurcation diagrams was carried out in the Poincaré section (P). To choose the appropriate Poincaré section, we used the general technique of setting one of the phase space coordinates to zero. In our analysis, we used the following condition

$$P\equiv max_R\{(R,\dot{R}):\dot{R}=0\}$$

which gives the maximal radius from each acoustic period. In addition, this condition was used to plot the bifurcation diagram of a cavitation bubble in [45,48]. This method continued through increasing the control parameter and the new resulting discrete points were plotted in the bifurcation diagrams versus the altered control parameters. For a full discussion on the bifurcation diagram, the Lyapunov exponent spectrum and their utilization in order to study the bubble dynamics, one can refer to [49–53].

4. Results and discussion

The organization of the article's results is as follows: first, the dynamics of bubbles in non-Newtonian fluids were explained using the standard methods of nonlinear dynamics, then the theory of deterministic chaos as well as the stability of bubbles under the influence of the viscoelasticity term, Deborah number, amplitude, and frequency of the acoustic pulse were mentioned. Next, our method for controlling the chaotic behavior of bubbles by applying a magnetic field is explained. Finally, an evaluation of our method in comparison to other similar chaos control methods is given.

The UCM method has been used in this study, since it is the most appropriate technique for the modeling of bubbles

Table 1
Constant parameters used in the general Rayleigh–Plesset equation [34,35].

Symbol	Description	Units	Value
σ	Fluid static surface tension	dyn/cm	55.89
ρ	Fluid density	kg/m^3	1060
p_0	Ambient pressure	atm	1
R_0	Equilibrium bubble radius	μm	1
Re	Reynolds number		2.5
k	Polytropic exponent		1.4

Table 2
Parameter ranges that used in this paper.

Parameter	Units	Range
De		2–7
P_a	Pa	1–10 ($\times 10^5$)
f	Hz	2.5–8 ($\times 10^6$)

in medical applications [34,35]. At $t = 0$, no pressure pulse is applied to the field and, thus, there is no shear stress distribution, and assuming $R(0) = 1$, equations will be solved in the coupled form (see Appendix B).

4.1. Presenting the dynamics of gas bubbles in viscoelastic fluids

Considering the general Rayleigh–Plesset equation, the stability of a bubble in a non-Newtonian fluid with respect to the Deborah number, pressure pulse amplitude, and pressure pulse frequency of the bubble has been studied. The result outlines a critical role of the control parameters in bubble dynamics and represents an outlook for the bubble dynamics complexity (All other physical parameters were kept constant at values given in Table 1).

4.1.1. The impact of the Deborah number

We examined the stability of a bubble in a non-Newtonian fluid by considering the Deborah number (De) of the bubble. Bubble growth to the initial radius of 1 μm, $Re = 2.5$ and $f = 3$ MHz, with various acoustic pressure amplitudes and frequencies, models the growth of bubbles in blood [35]. It can be stated that with the increase of the De number, bubble growth inside the blood fluid becomes chaotic, and due to instability, its control becomes impossible, so an elasticity threshold should be determined for the fluid. In addition, other researchers have reported the instability of time series with the increase of De [35,36,54], and a threshold of De for bubble stability could not be determined. The Radial motion of single bubble dynamics is investigated versus a prominent domain of De number from 2 to 7. In Fig 1. (a and d) the Deborah number interval is from 2 to 10 to illustrate the chaotic region clearly. Fig. 1 shows the bifurcation diagrams and the corresponding Lyapuonov spectrum, respectively, of the bubble radius when De number of the bubble is taken as the control parameter with the pressure amplitude of 200 and 400 kPa for several values of frequency of the external acoustic pressure (5 and 6 MHz) where stable and chaotic pulsations can be observed in each. There are windows of complex behavior with periods 4 oscillations in Fig. 1(a). This figure introduces intermittent chaotic and stable behaviors. After the first transition to chaos the bubble begins its stable oscillation with period four before its motion becomes chaotic for the another time. The maximum Lyapunov exponent is also an important indicator for a dynamic system for detecting potentially chaotic behavior. The maximum Lyapunov exponents are presented in Fig. 1(d–f) to verify the corresponding characteristics. In Fig. 1, we can detect a stable region, where the maximum Lyapunov exponent is always negative, and a chaotic region, where the Lyapunov exponent is mostly positive. These figures show that the chaotic radial oscillations of a bubble appeared by increasing the values of the De number, and the bubble demonstrates more chaotic radial oscillations as the frequency decreases.

4.1.2. The impact of the pressure pulse amplitude

In order to get more information about a bubble in a non-Newtonian fluid (for the purpose of finding periodic orbits and their stability), we plotted numerous bifurcation and maximum Lyapunov exponents diagrams of bubble radial oscillations considering several values for driving the pressure pulse amplitude P_a. Pressure pulse amplitude is a measure of the intensity of pulses applied to a bubble in a period. Due to the importance of pulse intensity in medical practices and the fact that these pulses should be applied to bubbles in order to collapse them in the blood stream [11], a proper value for the pulse intensity is used for determining and controlling the range of bubble stability. Here, these thresholds will be evaluated with respect to various frequencies and De

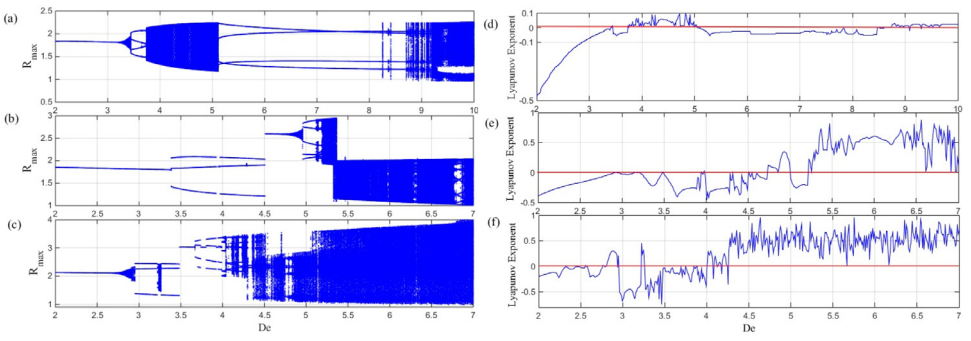

Fig. 1. Bifurcation diagrams and the corresponding Lyapuonov spectrum of bubble radius with 1 μm initial radius with versus Deborah number while the driving frequency and the pressure amplitude are (a) and (c) 5 MHz and 200 kPa, (b) and (e) 6 MHz and 400 kPa, (c) and (f) 5 MHz and 400 kPa, respectively.

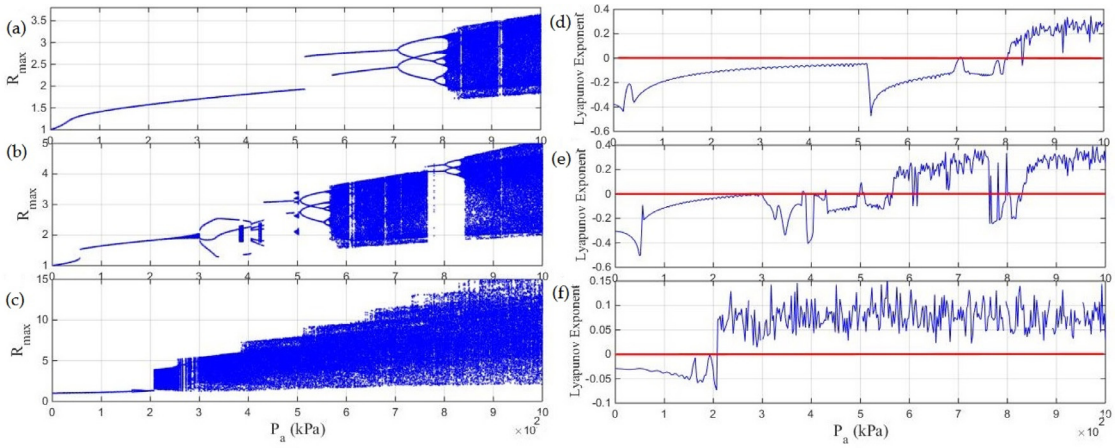

Fig. 2. Bifurcation diagrams and the corresponding Lyapuonov spectrum of bubble radius with 1 μm initial radius and Deborah number of 3 with versus pressure (10 kPa–1 MPa) while the driving frequency is (a) and (c) 7 MHz, (b) and (e) 5 MHz, (c) and (f) 3 MHz.

numbers, by plotting the bifurcation and Lyapunov exponents diagrams.

In Fig. 2, P_a has been considered as the control parameter while plotting the bifurcation and Lyapunov exponents diagrams, respectively. The chaotic effect of the pressure pulse amplitude on bubble dynamics is very clear. Considering Fig. 2(c) and (f), it can be concluded that at $P_a = 200$ kPa, the bubble's behavior becomes totally unstable. The effects of P_a as normal stresses at high frequencies lead to bubble stability and, thus, bubble radius reduction (see Fig. 2(a), (b), (d), and (e)). In addition, with the increase of P_a, bubble stability decreases. Fig. 2(c) also illustrates the transition through the instability threshold. However, due to the applied high frequency, this transition occurs at a larger P_a (see Fig. 2(a) and (b)). Comparing the Lyapunov exponents diagrams in Fig. 2(d–f) presented above, some limits of stable behavior could be determined for the bubble.

The results of Fig. 2 properly illustrate the effect of P_a on the degree of chaos in the system. Increasing P_a means applying greater normal stresses to the surface of the bubble which would simulate bubble growth. As Fig. 2 shows that, by increasing P_a, the stable range of the bubble decreases drastically, and the windows in the bifurcation diagrams are reduced. These results have also been verified in previous works [34–36]. As P_a is increased more, the possibility of a bubble collapse increases. Therefore, P_a control should be considered in medical applications. By comparing these figures, it can be found that the radial oscillation amplitude of bubble radius decreases considerably at high frequencies and low Deborah numbers, which could be due to the application of large pressure pulses on bubble surface at a shorter time. To carry drugs or genes to the goal sites, it is important to prevent the bubble from collapsing [11]. It can be concluded that the pressure pulse amplitude causes instabilities in the bubble's behavior, and this confirms the findings of other studies [34,35].

4.1.3. The impact of the pressure pulse frequency (f)

By considering the pressure pulse frequency as a control parameter, the application of a variety of pressure pulse frequencies on bubble dynamics has been studied (Fig. 3). In Fig. 3, bifurcation diagrams for the conditions of bubble growth in blood (conditions cited above) have been shown for various pressure pulse amplitudes and De numbers. The effects of frequency on bubble stability at various pressure pulse amplitudes and De numbers were evaluated. From these figures, it can be concluded that, with any increase in the pressure pulse frequency, the bubble becomes more stable and the bubble radius amplitude decreases considerably. According to the bubble growth equation, the frequency of the acoustic pulse is the main parameter in the fluctuations over the bubble interface. Most recently, dual forcing frequency methods of control (through applying a periodic perturbation [55]) have been proven to be successful in controlling the chaotic radial oscillations of bubbles. This method usually presents a technique based on using periodic perturbations to suppress the chaotic radial oscillations of spherical cavitation bubbles.

It can be understood from the results that the motions of bubbles can be chaotic or stable in particular ranges. The results are in agreement with the prior studies and clearly highlight that bubbles are dependent on the driving frequency variations [35,55–57]. Most of the results demonstrate the uncontrollable and chaotic motions in a bubble's dynamics. In dissimilar situations and values for controlling parameters (such as pressure, frequency and the Deborah number), a bubble shows various motions and radial oscillations and changes its motion from one type to another. This involves the transformation of a simple 'period one' by period doubling bifurcation to a 'period two' and then by successive period doublings to higher periods after which chaos occurs and the symmetry breaks.

4.2. Dynamics of gas bubbles in viscoelastic fluids in the presence of magnetic fields

In recent years, the explanation of the modern methods of nonlinear dynamic systems has been developed in recognizing the nonlinear behaviors of bubbles and encapsulated microbubbles [56–60]. Lately, researchers have been giving more attention to the investigation of these behaviors. It is believed that this phenomenon exhibits highly complex

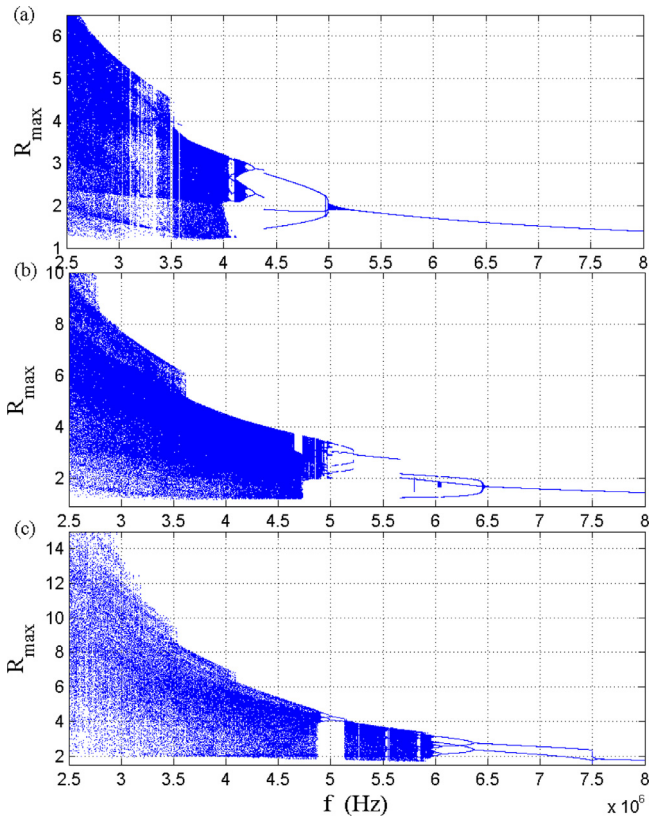

Fig. 3. Bifurcation diagrams of bubble radius with 1 μm initial radius with versus driving frequency (2.5 MHz–8 MHz) while: (a) Deborah number is 3 and $P_a = 300$ kPa, (b) Deborah number is 4 and $P_a = 400$ kPa, (c) Deborah number is 3 and $P_a = 600$ kPa.

and chaotic dynamics both numerically [56,57,61] and experimentally [62–64]. It is important to recognize the values of physical parameters determining chaotic radial oscillations, as this would be useful in defining the isolating field to enable the use of controlled bubbles in clinical applications. Most recently, the following methods of control have been proven to be successful in controlling chaotic radial oscillations of bubbles:

- Dual forcing frequency (through applying a periodic perturbation [55]).
- Varying bubble cluster size (the effects of coupling and bubble size [58]).

The first method uses periodic perturbation to suppress chaotic radial oscillations of a spherical cavitation bubble. The second method has theoretically focused on the suppression of chaos in the dynamics behavior of a small cluster of bubbles.

However, despite the extensive employment of the magnetic field in applications involving cavitation bubble phenomenon in viscoelastic fluids, there are no studies which estimate the proficiency of such control methods (which use magnetic fields) on a cavitation bubble system. In this paper, we intended to use proper control parameters to control the instability of the bubble system.

Our numerical simulation explicated that the radial oscillations of a bubble can have chaotic behavior. These results reveal that the chaotic radial oscillations of the bubble under the action of substantial parameters that influence the bubble dynamics can be used to distinguish stable and unstable regions of bubble pulsations and the expansion ratio of the bubble. In order to streamline the manifestation of the technique efficiency in suppressing chaos, a few chaotic zones have been chosen as samples to be subjected to the effects of the magnetic field. For the correlated zones, the dynamic behavior of the bubble was analyzed before and after the control process. This is done through computing its bifurcation diagram and the corresponding Lyapunov spectrum. Our goal is to seek Lyapunov exponents and bifurcation analysis to help us predict the dynamics of a bubble. The results are depicted in Figs. 4–7.

4.2.1. The effect of the Deborah number through applying a magnetic field

The first sample (Deborah number-bifurcation diagram of bubble when $B = 0$) is presented in Fig. 1(a). It belongs to a bubble with initial radius of 1 μm exposed to a frequency of the acoustic force of 5 MHz and with the pressure amplitude of 200 kHz when the control parameter is a Deborah number in the range of 2–7 (a condition used typically during the growth of bubble in blood [35]). It is easily understood that by increasing the Deborah number, the bubble stability is reduced and the obvious chaotic radial oscillations has been proven by previous studies [28,30,34–36,54].

In order to study the possibility of reducing chaos in bubble radial oscillation, a magnetic field is applied. Fig. 4(a–c)

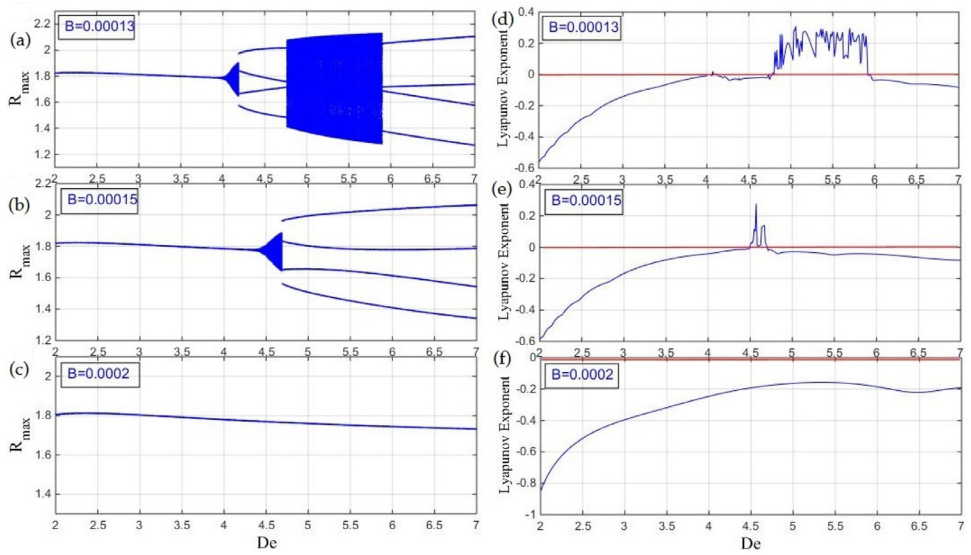

Fig. 4. Bifurcation diagrams and the corresponding Lyapuonov spectrum of bubble radius with 1 μm initial radius, 200 kPa pressure and frequency of 5 MHz with versus Deborah number (2–7) while the magnetic field is (a) and (c) 0.00013, (b) and (e) 0.00015, (c) and (f) 0.0002.

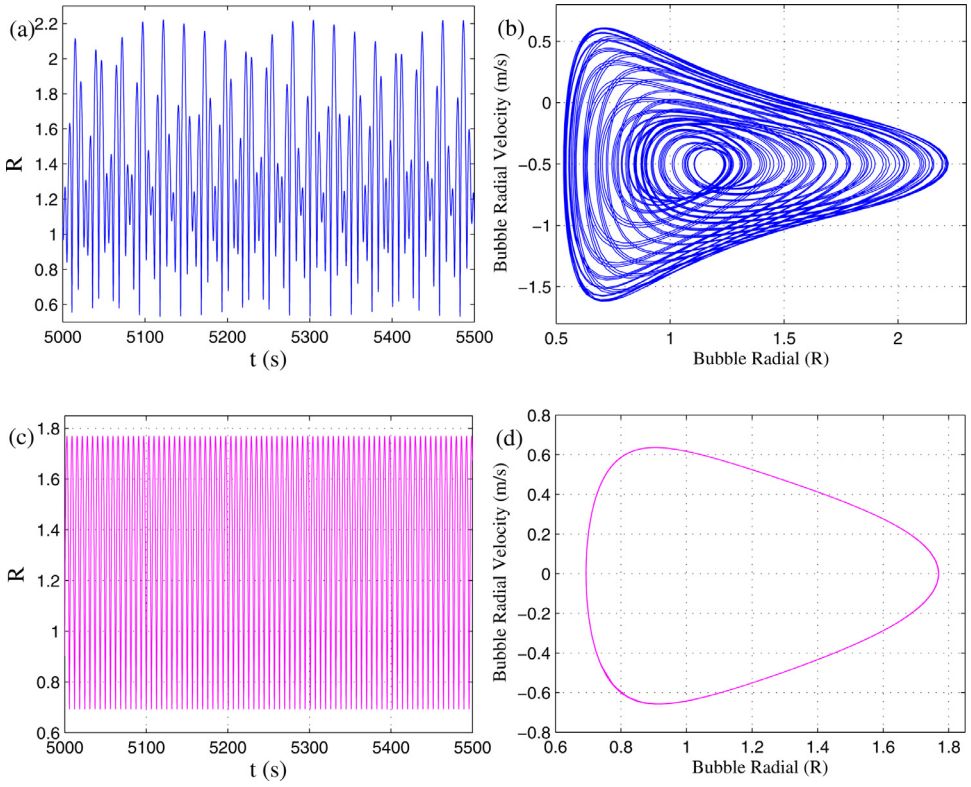

Fig. 5. Time series and trajectory in state space projection of bubble radius driven by 4.5 Deborah number, 200 kPa of pressure and frequency of 5 MHz: (a,b) chaotic oscillations (Without applying the magnetic field), (c,d) regular oscillations (after applying the magnetic field $B = 0.0002$).

give us some information about controlling dynamics after applying the magnetic field ($B = 0.00013,\ 0.00015$ and 0.0002). After the employment of these methods, it was observed that the chaotic zone is reduced (see Fig. 4(a and b)). The maximum Lyapunov exponent is also an important indicator for a dynamic system for detecting potentially chaotic behavior. Accordingly, the maximum Lyapunov exponents is outlined in Fig. 4(d–f). Fig. 1(d) introduces the original system, while Fig. 4(d–f) introduces the controlled system, where the Lyapunov exponent is mostly positive

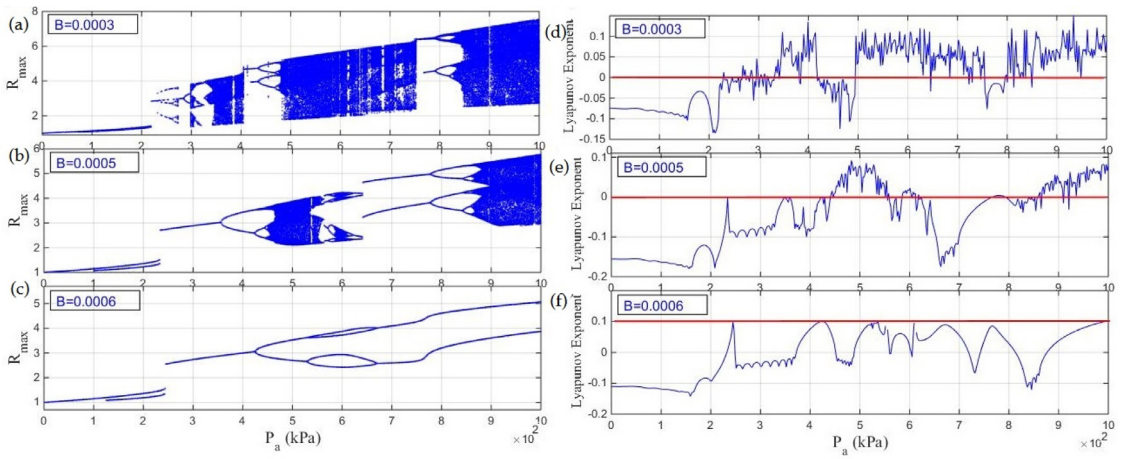

Fig. 6. Bifurcation diagrams and the corresponding Lyapuonov spectrum of bubble radius with 1 μm initial radius, frequency of 5 MHz and Deborah number of 3 with versus pressure (10 kPa–1 MPa) while the magnetic field is (a) and (c) 0.0003, (b) and (e) 0.0005, (c) and (f) 0.0006.

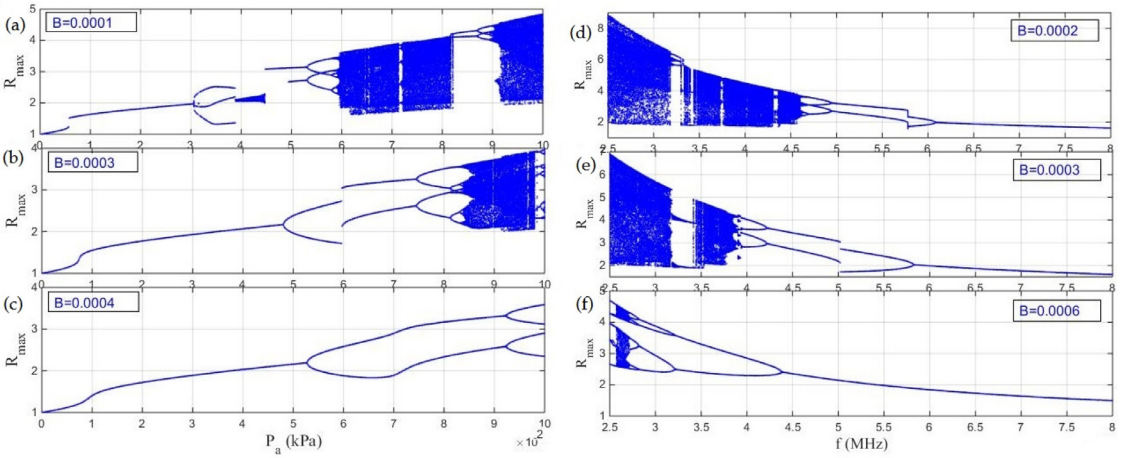

Fig. 7. (a–c) Bifurcation diagrams of bubble radius with 1 μm initial radius, frequency of 3 MHz and Deborah number of 3 with versus pressure (10 kPa–1 MPa) while the magnetic field is (a) 0.0001, (b) 0.0003, (c) 0.0004. (d–f) Bifurcation diagrams of bubble radius with 1 μm initial radius, pressure of 600 kPa and Deborah number of 3 with versus frequency (2.5 MHz–8 MHz) while the magnetic field is (d) 0.0002, (e) 0.0003 and (f) 0.0006.

showing a chaotic behavior. The negative Lyapunov exponent demonstrates the stable behavior. In order to better understand the magnetic field control method, Fig. 5 shows a plot of the bubble radial oscillations versus time in a certain pressure value before and after the control. Figs. 4 and 5 show how the application of the magnetic field leads to the reduction of the chaotic radial oscillations to periodic oscillations under various Deborah numbers.

4.2.2. The effect of the acoustic pressure through applying a magnetic field

By considering the acoustic pressure as a control parameter (a condition typically used during the growth of bubble in blood [35]), the effect of varying the acoustic pressure through applying the magnetic field on bubble dynamics has been studied. Fig. 2(b) shows the second chaotic sample zone (pressure bifurcation diagram of bubble) before applying the magnetic field ($B = 0$). It is related to a bubble subjected to a driving frequency source of 3 MHz and a Deborah number 3 versus its acoustic pressure as the control parameter. When the acoustic pressure (P_a) is used as the control parameter, a period doubling sequence is followed by a transition to chaos. Fig. 6(a–c) demonstrates the controlled dynamics through applying the magnetic field ($B =$ 0.0003, 0.0005 and 0.0006). As seen, the magnetic field had an impact on the dynamics and has regulated the undulations in Fig. 6(a–c). Although the patterns of the radial oscillations and their maximum amplitudes are slightly different, applying the stated magnetic field provides a suitable control over the chaotic radial oscillations of Fig. 2(b). The effects of the magnetic field are also tested through the maximum Lyapunov exponents diagrams (see Fig. 6(d–f)). This figure illustrates a significant decrease in the maximum Lyapunov exponents from positive values to negative ones indicating that stable behaviors were achieved when the applied magnetic field was engaged. Fig. 2(f) corresponds to the original bubble dynamics system ($B = 0$), and Fig. 7 corresponds to the controlled system after applying the magnetic field

($B = 0.0001,\ 0.0003$ and 0.0004). The obtained results indicate that stable dynamics can be achieved after applying the proposed technique.

4.2.3. The effect of the pressure pulse frequency through applying a magnetic field

In order to study the dynamic response of the system to the perturbation induced by the magnetic field, not only the effect of the Deborah number and acoustic pressure, but also its frequency should be considered. The effect of the magnetic field on bubble radial oscillation was studied for different models. In order to streamline the manifestation of the magnetic field efficiency in suppressing chaos, third chaotic zones have been chosen as samples to be subjected to the effect of the pressure pulse frequency through applying the magnetic field. For the associated zone, the dynamic behavior of the bubble was analyzed before and after applying the magnetic field, and this was done by computing its bifurcation diagrams versus the value of the magnetic field. Fig. 3 shows the bifurcation diagrams of the bubble radius when the frequency of the bubble is taken as the control parameter for $B = 0$ with several values of the Deborah number and acoustic pressure of the bubble where stable and chaotic pulsations can be observed in each. The third sample zone (frequency bifurcation diagram of bubble when $B = 0$) is presented in Fig. 3(c). It belongs to a bubble with initial radius of 1 μm exposed to an acoustic pressure of 600 kPa when the control parameter is a frequency in the range of 2.5 MHz–8 MHz. In order to study the possibility of reducing chaos, various magnetic fields are applied. Fig. 7(d–f) presents the controlled dynamics after applying the magnetic field. It is shown that applying the magnetic field reduces the chaotic zone (see Fig. 7(f)).

It is necessary to have a good understanding of the bubble dynamics to provide reliable control mechanisms for the wide range of applications in industry. A better understanding of bubbles' behavior is the first step towards controlling chaotic behavior of the bubble and using cavitation. Reducing chaos using magnetic fields can be practically advantageous, particularly in applications involving bubbles for medical purposes. For instance, chaotic radial oscillations of the bubbles decrease the treatment efficacy and make it difficult to control. Reducing chaotic dynamics can be the first step in increasing the predictability and safety of the treatment.

5. Conclusion and outlook

In this paper, bubble stability dynamics in non-Newtonian fluids have been illustrated using techniques of chaos physics. In the presence of a magnetic field, ranges in which a bubble assumes a stable behavior have been shown by diagrams. The results indicate that applying a magnetic field to the bubble eliminates typical instabilities. Furthermore, the results also indicate that the Deborah number, a measure of the non-Newtonian state of the fluid, severely affects the bubble stability; with the increase in Deborah number, the bubble experiences irregular radial oscillations. These findings confirm the results reported in [28,30,34–36,54]. In view of this fact, the injection and conveyance of bubbles in the blood stream should be performed very carefully, and the non-Newtonian state of blood should be tested and measured.

In addition, according to the presented diagrams, the increase of the acoustic pressure amplitude causes instability in the bubble boundary and may lead to bubble collapse. This finding has also been pointed out in the articles of Allen and Roy and Jimenez-Fernandez and Crespo [34–36]. Moreover, by increasing the acoustic wave frequency, which indicates the number of pressure pulses in a time unit, the surface of the bubble could be subjected to pressure force, and its irregular radial oscillations could be avoided. In this article, it has been demonstrated that the increase in the pressure pulse frequency causes the radial oscillation amplitude to decrease and leads to bubble stability.

In this paper, our main contribution is the development of the effect of the magnetic field on nonlinear pulsations of a spherical bubble to control the chaotic behavior of bubble dynamics. It is shown that the magnetic field has the ability to control the behavior of the bubble. Parameter B allows us to control the chaotic region and modify the lengths of the unstable region. Therefore, we can select a corresponding control process to match our physical conditions. Focusing on the mechanisms governing the transition from the chaotic radial oscillations to the stable region, this study opens a new view in studying the chaotic control behavior of the nonlinear dynamics of the bubble in non-Newtonian fluids. Once more, it should be mentioned that controlling the chaotic radial oscillations of bubbles is studied through applying the magnetic field. This method is simple and easy to implement experimentally. It is essential to consider the bubble–bubble interaction in choosing the control parameter since the bubble pulsation is affected by interacting with the surrounding bubbles [65,66]. In general, the introduced method can be used for studying the behavior of the cluster with a large number of bubbles.

Appendix A. Governing equations with magnetic field

The mass conservation equation in the liquid can be expressed as

$$\frac{\partial \rho}{\partial t} + \bar{\nabla} \cdot (\rho \bar{u}) = 0 \tag{A.1}$$

where $\bar{u}$ is the liquid particle velocity. Furthermore, the momentum conservation equation in liquid is defined as

$$\rho \frac{D\bar{u}}{Dt} = \rho \left(\frac{\partial \bar{u}}{\partial t} + (\bar{u} \cdot \bar{\nabla})\bar{u} \right) = \rho \sum \bar{F}_{ext} - \bar{\nabla} p + \frac{\bar{\tau}_{rr} - \bar{\tau}_{\theta\theta}}{r} - \sigma B^2 \bar{u} \tag{A.2}$$

If assumed that the bubble always will remain in spherical shape, then because of the symmetry in the infinite surrounding liquid domain, the liquid particle velocity will be $u(r, t)$ which is always in radial direction and the conservation equations will reduce to

$$\frac{\partial \rho}{\partial t} + \frac{1}{r^2} \frac{\partial (r^2 \rho u)}{\partial r} = 0 \tag{A.3}$$

and

$$\frac{\partial u}{\partial t} + u \frac{\partial u}{\partial r} + \frac{1}{\rho} \frac{\partial p}{\partial r} + \frac{\sigma B^2 u}{\rho} - \frac{\tau_{rr} - \tau_{\theta\theta}}{\rho r} = 0 \tag{A.4}$$

where τ_{rr} and $\tau_{\theta\theta}$ terms can be found from Eq. (2). Following the derivation of modified Rayleigh–Plesset equation and by using Eq. (A.3) with wave equation for velocity potential Φ, the mass conservation equation in an incompressible flow will reduce to:

$$\nabla^2\Phi = 0 \tag{A.5}$$

which yields into:

$$\Phi(r,t) = -\frac{R^2\dot{R}}{r} \tag{A.6}$$

After simplifying, the momentum conservation equation can be rewritten as

$$\frac{\partial\Phi(r,t)}{\partial r} + \frac{1}{2}\left(\frac{\partial\Phi(r,t)}{\partial r}\right)^2 = -\frac{p(r,t)-p_0-P(t)}{\rho} - \frac{\sigma B^2\Phi(r,t)}{\rho} + \int_r^{r_1}\frac{\tau_{rr}-\tau_{\theta\theta}}{\rho r'}dr' = 0 \tag{A.7}$$

Also, by simplifying at $r = R$ (Bubble wall), the momentum equation will reduces to:

$$R\ddot{R} + \frac{3\dot{R}^2}{2} = \frac{P_L(t)-p_0-P(t)}{\rho} - \frac{\sigma B^2}{\rho}R\dot{R} + \int_r^{r_1}\frac{\tau_{rr}-\tau_{\theta\theta}}{\rho r'}dr' \tag{A.8}$$

Using the assumptions made by Rayleigh, the GRP equation with acoustic forced oscillation can be rewritten as

$$R\ddot{R} + \frac{3\dot{R}^2}{2} + \frac{\sigma B^2}{\rho}R\dot{R} = \frac{1}{\rho}\left[\rho_{g_0}\left(\frac{R_0}{R}\right)^{3k} - (p_0 + p_A\sin\omega t) - \frac{2\sigma_s}{R} + \int_r^{r_1}\frac{\tau_{rr}-\tau_{\theta\theta}}{r'}dr'\right] \tag{A.9}$$

Appendix B. Algebric calculations

Eqs. (4) and (5) can thus be expressed as a system of first-order ordinary differential equations in which the zero point is located on the wall of the spherical bubble:

$$\begin{cases} \frac{dR}{dt} = U, \\ \frac{dU}{dt} = \left[-\frac{3}{2}U^2 + \frac{p_0}{\rho\omega^2R_0^2}\left((1+We)\left(\frac{1}{R}\right)^{3k} - We\left(\frac{1}{R}\right) - (1+\alpha\sin(t))\right)\right]\frac{1}{R} \\ \quad + \frac{1}{R}\frac{2}{3Re}\left(\frac{1}{\omega R_0}\sqrt{\frac{p_0}{\rho}}\right)\times\int_0^{\infty}\left(\frac{\tau_{rr}(y,t)-\tau_{\theta\theta}(y,t)}{y_i+R^3}\right)dy - \frac{\sigma B^2}{\rho}U, \\ \frac{d\tau_{rr}(y.t)}{dt} = \left(\left(\frac{-4R^2\dot{R}}{y_i+R^3}\right) - \frac{1}{De}\right)\tau_{rr} + \frac{4}{De}(\omega R_0\sqrt{\frac{p_0}{\rho}})\left(\frac{R^2\dot{R}}{y_i+R^3}\right), \\ \frac{d\tau_{\theta\theta}(y.t)}{dt} = \left(\left(\frac{2R^2\dot{R}}{y_i+R^3}\right) - \frac{1}{De}\right)\tau_{rr} - \frac{2}{De}(\omega R_0\sqrt{\frac{p_0}{\rho}})\left(\frac{R^2\dot{R}}{y_i+R^3}\right). \end{cases} \tag{B.1}$$

We is the Weber number, defined as

$$We = \frac{2\sigma}{p_cR_0} \tag{B.2}$$

Also, in above equation the initial conditions are taken as

$$R(0) = 1, \tag{B.3}$$

$$\tau_{\theta\theta}(0) = \tau_{rr}(0) = 0 \tag{B.4}$$

$$U(0) = 0. \tag{B.5}$$

This study is conducted for De $\sim O(1)$ to avoid numerical difficulties that arise from the division by this quantity in Eq. (B.1). The following assumptions have been adopted:

1. The material outside the gas bubble wall is incompressible.
2. The bubble remains spherical.
3. The spatially uniform conditions are assumed to exist within the bubble.
4. The convective term of material derivative of particle velocity is zero.
5. The magnetic field is constant.

References

[1] Rayleigh L. VIII. On the pressure developed in a liquid during the collapse of a spherical cavity. Lond Edinb Dublin Philos Mag J Sci 1917;34:94–8.
[2] Plesset M. The dynamics of cavitation bubbles. J Appl Mech 1949;16:227–82.
[3] Plesset M. On the stability of fluid flows with spherical symmetry. J Appl Phys 1954;25:96–8.
[4] Crum LA, Eller AI. Motion of bubbles in a stationary sound field. J Acoust Soc Am 1970;48:181–9.
[5] Flynn HG. Cavitation dynamics. I. A mathematical formulation. J Acoust Soc Am 1975;57:1379–96.
[6] Lauterborn W. Numerical investigation of nonlinear oscillations of gas bubbles in liquids. J Acoust Soc Am 1976;59:283–93.
[7] Plesset MS, Prosperetti A. Bubble dynamics and cavitation. Annu Rev Fluid Mech 1977;9:145–85.
[8] Prosperetti A. The equation of bubble dynamics in a compressible liquid. Phys Fluids 1987;30:3626–8.
[9] Prosperetti A. Bubble dynamics: some things we did not know 10 years ago (Bubble dynamics and interface phenomena). Springer; 1994. p. 3–16.
[10] Prosperetti A, Lezzi A. Bubble dynamics in a compressible liquid. Part 1. First-order theory.. J Fluid Mech 1986;168:457–78.
[11] Suzuki R, Takizawa T, Negishi Y, Utoguchi N, Maruyama K. Effective gene delivery with novel liposomal bubbles and ultrasonic destruction technology. Int J Pharm 2008;354:49–55.
[12] Hernot S, Klibanov AL. Microbubbles in ultrasound-triggered drug and gene delivery. Adv Drug Deliv Rev 2008;60:1153–66.
[13] Ibsen S, Benchimol M, Simberg D, Schutt C, Steiner J, Esener S. A novel nested liposome drug delivery vehicle capable of ultrasound triggered release of its payload. J Control Release 2011;155:358–66.
[14] Husseini GA, de la Rosa MAD, Richardson ES, Christensen DA, Pitt WG. The role of cavitation in acoustically activated drug delivery. J Control Release 2005;107:253–61.
[15] Frenkel V. Ultrasound mediated delivery of drugs and genes to solid tumors. Adv Drug Deliv Rev 2008;60:1193–208.
[16] Hynynen K. Ultrasound for drug and gene delivery to the brain. Adv Drug Deliv Rev 2008;60:1209–17.
[17] Suzuki R, Namai E, Oda Y, Nishiie N, Otake S, Koshima R, Hirata K, Taira Y, Utoguchi N, Negishi Y, et al. Cancer gene therapy by IL-12 gene delivery using liposomal bubbles and tumoral ultrasound exposure. J Control Release 2010;142:245–50.
[18] Johnston BM, Johnston PR, Corney S, Kilpatrick D. Nonnewtonian blood flow in human right coronary arteries: transient simulations. J Biomech 2006;39:1116–28.
[19] Janela J, Moura A, Sequeira A. A 3d non-Newtonian fluid-structure interaction model for blood flow in arteries. J Comput Appl Math 2010;234:2783–91.
[20] Ashrafizaadeh M, Bakhshaei H. A comparison of non-Newtonian models for lattice Boltzmann blood flow simulations. Comput Math Appl 2009;58:1045–54.
[21] Wang C-H, Ho J-R. A lattice Boltzmann approach for the non-Newtonian effect in the blood flow. Comput Math Appl 2011;62:75–86.
[22] Favelukis M, Albalak RJ. Bubble growth in viscous newtonian and non-newtonian liquids. Chem Eng J Biochem Eng J 1996;63:149–55.
[23] Jiang S, Ma Y, Fan W, Yang K, Li H. Chaotic characteristics of bubbles rising with coalescences in pseudoplastic fluid. Chin J Chem Eng 2010;18:18–26.

[24] Schembri F, Sapuppo F, Bucolo M. Experimental classification of nonlinear dynamics in microfluidic bubbles flow. Nonlinear Dyn 2012;67:2807–19.
[25] Ichihara M, Ohkunitani H, Ida Y, Kameda M. Dynamics of bubble oscillation and wave propagation in viscoelastic liquids. J Volcanol Geotherm Res 2004;129:37–60.
[26] Fu T, Ma Y, Funfschilling D, Li HZ. Bubble formation in nonnewtonian fluids in a microfluidic t-junction. Chem Eng Process: Process Intensif 2011;50:438–42.
[27] Frank X, Dietrich N, Wu J, Barraud R, Li HZ. Bubble nucleation and growth in fluids. Chem Eng Sci 2007;62:7090–7.
[28] Kafiabad HA, Sadeghy K. Chaotic behavior of a single spherical gas bubble surrounded by a giesekus liquid: a numerical study. J Non-Newtonian Fluid Mech 2010;165:800–11.
[29] Li HZ, Mouline Y, Midoux N. Modelling the bubble formation dynamics in non-newtonian fluids. Chem Eng Sci 2002;57:339–46.
[30] Jiménez-Fernández J, Crespo A. The collapse of gas bubbles and cavities in a viscoelastic fluid. Int J Multiph flow 2006;32:1294–9.
[31] Li HZ, Frank X, Funfschilling D, Mouline Y. Towards the understanding of bubble interactions and coalescence in non-newtonian fluids: a cognitive approach. Chem Eng Sci 2001;56:6419–25.
[32] Bloom F. Bubble stability in a class of non-Newtonian fluids with shear dependent viscosities. Int J Non-linear Mech 2002;37:527–39.
[33] Wang H-m, Jiang X-p, Ma J-m, Zhang W. Vibration of a single protein bubble in bingham liquid. J Hydrodyn Ser B 2009;21:658–68.
[34] Allen JS, Roy RA. Dynamics of gas bubbles in viscoelastic fluids. I. Linear viscoelasticity. J Acoust Soc Am 2000a;107:3167–78.
[35] Allen JS, Roy RA. Dynamics of gas bubbles in viscoelastic fluids. II. Nonlinear viscoelasticity. J Acoust Soc Am 2000b;108:1640–50.
[36] Jiménez-Fernández J, Crespo A. Bubble oscillation and inertial cavitation in viscoelastic fluids. Ultrasonics 2005;43:643–51.
[37] Lind SJ, Phillips TN. Spherical bubble collapse in viscoelastic fluids. J Non-Newtonian Fluid Mech 2010;165:56–64.
[38] Brujan E-A. A first-order model for bubble dynamics in a compressible viscoelastic liquid. J Non-newtonian Fluid Mech 1999;84:83–103.
[39] Sorokin V, Blekhman I, Thomsen JJ. Motions of elastic solids in fluids under vibration. Nonlinear Dyn 2010;60:639–50.
[40] Sorokin V, Blekhman I, Vasilkov V. Motion of a gas bubble in fluid under vibration. Nonlinear Dyn 2012;67:147–58.
[41] Aliabadi A, Taklifi A. The effect of magnetic field on dynamics of gas bubbles in visco-elastic fluids. Appl Math Model 2012;36:2567–77.
[42] Siewe MS, Yamgoue S, Kakmeni FM, Tchawoua C. Chaos controlling self-sustained electromechanical seismograph system based on the melnikov theory. Nonlinear Dyn 2010;62:379–89.
[43] Gao Q, Ma J. Chaos and hopf bifurcation of a finance system. Nonlinear Dyn 2009;58:209–16.
[44] Chen H, Zuo D, Zhang Z, Xu Q. Bifurcations and chaotic dynamics in suspended cables under simultaneous parametric and external excitations. Nonlinear Dyn 2010;62:623–46.
[45] Jiménez-Fernández J. Dynamics of gas bubbles encapsulated by a viscoelastic fluid shell under acoustic fields. Acta Acust United Acust 2014;100:1024–35.
[46] Strogatz SH. Nonlinear dynamics and chaos: with applications to physics, biology, chemistry, and engineering. Westview Press; 2014.
[47] Behnia S, Yahyavi M. Characterization of intermittency in hierarchy of chaotic maps with invariant measure. J Phys Soc Jpn 2012;81:124008-8.
[48] Simon G, Cvitanovic P, Levinsen M, Csabai I, Horvath A. Periodic orbit theory applied to a chaotically oscillating gas bubble in water. Nonlinearity 2002;15:25.
[49] Parlitz U, Englisch V, Scheffczyk C, Lauterborn W. Bifurcation structure of bubble oscillators. J Acoust Soc Am 1990;88:1061–77.
[50] Lauterborn W, Parlitz U. Methods of chaos physics and their application to acoustics. J Acoust Soc Am 1988;84:1975–93.
[51] Kooi BW, Aguiar M, Stollenwerk N. Analysis of an asymmetric two-strain dengue model. Math Biosci 2014;248:128–39.
[52] McLennan-Smith TA, Mercer GN. Complex behaviour in a dengue model with a seasonally varying vector population. Math Biosci 2014;248:22–30.
[53] Upadhyay RK, Raw SN, Roy P, Rai V. Restoration and recovery of damaged eco-epidemiological systems: application to the Salton Sea, California, USA. Math Biosci 2013;242:172–87.
[54] Albernaz D, Cunha F. Bubble dynamics in a maxwell fluid with extensional viscosity. Mech Res Commun 2011;38:255–60.
[55] Behnia S, Sojahrood AJ, Soltanpoor W, Jahanbakhsh O. Suppressing chaotic oscillations of a spherical cavitation bubble through applying a periodic perturbation. Ultrason Sonochem 2009;16:502–11.
[56] Macdonald C, Gomatam J. Chaotic dynamics of microbubbles in ultrasonic fields. J Mech Eng Sci Proc IMechE 2006;220:333–43.
[57] Behnia S, Jafari A, Soltanpoor W, Jahanbakhsh O. Nonlinear transitions of a spherical cavitation bubble. Chaos Solitons Fractals 2009;41:818–28.
[58] Chong K, Quek C, Dzaharudin F, Ooi A, Manasseh R. The effects of coupling and bubble size on the dynamical-systems behaviour of a small cluster of microbubbles. J Sound Vib 2010;329:687–99.
[59] Stride E, Tang M, Eckersley R. Physical phenomena affecting quantitative imaging of ultrasound contrast agents. Appl Acoust 2009;70:1352–62.
[60] Jiménez-Fernández J. Nonlinear response to ultrasound of encapsulated microbubbles. Ultrasonics 2012;52:784–93.
[61] Akhatov IS, Konovalova S. Regular and chaotic dynamics of a spherical bubble. J Applied Math Mech 2005;69:575–84.
[62] Lauterborn W, Cramer E. Subharmonic route to chaos observed in acoustics. Phys Rev Lett 1981;47:1445–8.
[63] Lauterborn W, Koch A. Holographic observation of period-doubled and chaotic bubble oscillations in acoustic cavitation. Phys Rev A 1987;35:1974–6.
[64] Holt RG, Gaitan DF, Atchley AA, Holzfuss J. Chaotic sonoluminescence. Phys Rev Lett 1994;72:1376–9.
[65] Yasui K, Iida Y, Tuziuti T, Kozuka T, Towata A. Strongly interacting bubbles under an ultrasonic horn. Phys Rev E 2008;77:016609–19.
[66] Behnia S, Zahir H, Yahyavi M, Barzegar A, Mobadersani F. Observations on the dynamics of bubble cluster in an ultrasonic field. Nonlinear Dyn 2013;72:561–74.